Synthetic and Systems Biotechnology 9 (2024) 834–841

Contents lists available at ScienceDirect

Synthetic and Systems Biotechnology

journal homepage: www.keaipublishing.com/en/journals/synthetic-and-systems-biotechnology

Original Research Article

Synergistic increase in coproporphyrin III biosynthesis by mitochondrial compartmentalization in engineered *Saccharomyces cerevisiae*

Qidi Guo [a], Jiaqi Xu [a,c], Jiacun Li [a], Shuyan Tang [a], Yuhui Cheng [a], Bei Gao [a], Liang-Bin Xiong [c,**], Jie Xiong [b,***], Feng-Qing Wang [a,*], Dong-Zhi Wei [a]

[a] State Key Lab of Bioreactor Engineering, Newworld Institute of Biotechnology, East China University of Science and Technology, Shanghai, 200237, China
[b] Department of Gastroenterology, Tongji Institute of Digestive Disease, Tongji Hospital, School of Medicine, TongJi University, Shanghai, 200065, China
[c] Shanghai Key Laboratory of Molecular Imaging, School of Pharmacy, Shanghai University of Medicine and Health Sciences, Shanghai, 201318, China

ARTICLE INFO

Keywords:
Coproporphyrin III
Saccharomyces cerevisiae
Mitochondrial compartmentalization
Anti-oxidation

ABSTRACT

Coproporphyrin III (CP III), a natural porphyrin derivative, has extensive applications in the biomedical and material industries. *S. cerevisiae* has previously been engineered to highly accumulate the CP III precursor 5-aminolevulinic acid (ALA) through the C4 pathway. In this study, a combination of cytoplasmic metabolic engineering and mitochondrial compartmentalization was used to enhance CP III production in *S. cerevisiae*. By integrating pathway genes into the chromosome, the CP III titer gradually increased to 32.5 ± 0.5 mg/L in shake flask cultivation. Nevertheless, increasing the copy number of pathway genes did not consistently enhance CP III synthesis. Hence, the partial synthesis pathway was compartmentalized in mitochondria to evaluate its effectiveness in increasing CP III production. Subsequently, by superimposing the mitochondrial compartmentalization strategy on cytoplasmic metabolic engineered strains, the CP III titer was increased to 64.3 ± 1.9 mg/L. Furthermore, augmenting antioxidant pathway genes to reduce reactive oxygen species (ROS) levels effectively improved the growth of engineered strains, resulting in a further increase in the CP III titer to 82.9 ± 1.4 mg/L. Fed-batch fermentations in a 5 L bioreactor achieved a titer of 402.8 ± 9.3 mg/L for CP III. This study provides a new perspective on engineered yeast for the microbial production of porphyrins.

1. Introduction

Porphyrins exhibit diverse functional properties and have been used in various biomedical fields, including tumor inhibition, drug targeting and photodynamic therapy [1–3]. In addition, their distinctive molecular structure endows them with exceptional optical properties, making them one of the most promising photochemical materials for use in solar cells, solid–liquid interfaces and chemical sensors [4–9]. For instance, heme is a porphyrin molecule present in blood that acts as a soluble redox catalyst to facilitate battery charging by accepting and releasing free oxygen species [7]. Cu(II) and Zn(II) coproporphyrins can serve as sensitizers in fuel-sensitized solar cells [10], while Zn(II) coproporphyrins also demonstrate excellent supramolecular photosensitizers and possess potent antibacterial activity [11].

The synthesis of porphyrins in industrial production commonly involves the use of chemical methods [12,13]. However, the complex synthesis steps contribute to increased production costs and render porphyrins highly expensive. Moreover, chemically synthesized porphyrins lack the desired stereoselectivity and regioselectivity. Consequently, a more economical, sustainable, eco-friendly, and effective method to produce porphyrins is required. In recent years, microbial cell factories have emerged as effective alternatives for producing natural products and high-value chemicals by feeding low-cost precursors such as glucose. *S. cerevisiae* is a well-established cell factory that can be used to produce fuels [14], chemicals [15,16] and heterologous proteins [17].

Abbreviations: ALA, 5-aminolevulinic acid; CP III, coproporphyrin III; PP IX, protoporphyrin IX; MLS, mitochondrial localization signal; ROS, reactive oxygen species; GSH, glutathione; SOD, superoxide dismutase; CAT, catalase.

Peer review under responsibility of KeAi Communications Co., Ltd.

* Corresponding author.
** Corresponding author.
*** Corresponding author.
E-mail addresses: xionglb@sumhs.edu.cn (L.-B. Xiong), doctorxiongj@163.com (J. Xiong), fqwang@ecust.edu.cn (F.-Q. Wang).

https://doi.org/10.1016/j.synbio.2024.07.001
Received 15 May 2024; Received in revised form 4 July 2024; Accepted 10 July 2024
Available online 14 July 2024

Unlike prokaryotes, *S. cerevisiae* possesses multiple organelles that can provide distinct environments and compartments for biosynthesis processes, and exhibits remarkable tolerance to harsh industrial conditions [18,19]. In *S. cerevisiae*, porphyrin biosynthesis primarily occurs through the heme biosynthesis pathway which spans both mitochondria and cytoplasmic [20]. The synthesis of ALA is the first step in heme biosynthesis, which is followed by four or five steps of enzymatic reactions to yield coproporphyrin III (CP III) or protoporphyrin IX (PP IX). These two porphyrins can serve as precursors for various derivatives; however, only limited studies have been conducted on enhancing their accumulation in engineered *S. cerevisiae* strains [20,21]. Although porphyrin production has been observed in engineered *S. cerevisiae* strains, the yield remains relatively low and few reports have focused on coproporphyrin III production.

As multifunctional suborganelles in eukaryotic cells, mitochondria can serve as sites for various metabolic processes, including the tricarboxylic acid cycle, oxidative phosphorylation, amino acid and lipid metabolism, and the synthesis of iron-sulfur clusters and heme [22]. Organelle engineering has been widely recognized as an effective method for improving the yield of target products in *S. cerevisiae* owing to the distinct advantages of highly specialized suborganelles, such as a plentiful supply of precursors and cofactors, compartmentalization of metabolic pathways and suitable biochemical environments for enzyme and product storage [23–25]. The feasibility of utilizing mitochondria for efficient synthesis of high value-added products has been extensively studied. Yee et al. demonstrated that targeting the geraniol biosynthesis pathway to yeast mitochondria resulted in a 6-fold increase in yield, suggesting that mitochondria can serve as an effective suborganelle for monoterpene production [26]. By systematic metabolic engineering of the sabinene biosynthetic pathway in the cytoplasm and mitochondria, a 60-fold increase of the sabinene titer was achieved compared to the original strain [27]. Recently, we demonstrated that mitochondria can be employed as a highly efficient suborganelle for the synthesis of squalene, resulting in a remarkable increase in the squalene titer to 21.1 g/L through cytoplasmic and mitochondrial engineering via two-stage fed-batch fermentation [28]. These studies substantiated that mitochondria were a potential organelle for the compartmentalization pathways in yeasts.

In this study, we investigated the synergistic improvement effect of mitochondrial compartmentalization combined with cytoplasmic metabolic engineering on CP III production in *S. cerevisiae*. First, additional a copy of pathway genes was implanted into chromosomes to enhance CP III synthesis. After determining that increasing the copy number of pathway genes has limited effect on improving CP III synthesis, we tested the effect of mitochondrial compartmentalization on CP III synthesis. Subsequently, the synergistic effect of cytoplasmic engineering combined with mitochondrial engineering on enhancing CP III accumulation was examined. In addition, genes implicated in reducing cellular reactive oxygen species (ROS) levels were overexpressed to improve cell growth and physiology, thus achieving better CP III accumulation.

2. Materials and methods

2.1. Strains, media and reagents

S. cerevisiae CEN. PK2–1C *(MATa; ura3-52; trp1-289; leu2-3, 112; his3Δ1; MAL2-8^{C}; SUC2)* was used as the host for engineering. All yeast strains used in this study are listed in Table 1. *Escherichia coli* DH5α (NCM Biotech, Suzhou, Jiangsu, China) was used for gene cloning. Luria–Bertani (LB) broth supplemented with antibiotics (100 μg/mL ampicillin) was used for the cultivation of recombinant *E. coli*. YPD medium (10.0 g/L yeast extract, 20.0 g/L peptone and 20.0 g/L glucose, pH 7.0) was used for cultivation of the yeast strains. The selection of yeast strains with pTCL, a Cas9 protein expression plasmid, was performed using SD-Leu (synthetic complete drop-out medium containing 2 % D-glucose and lacking leucine). SD-Leu-Ura (synthetic complete drop-out medium with 2 % D-glucose and without leucine and uracil) was used for the selection of yeast strains with both the Cas9 protein expression plasmid and guide RNA (gRNA) plasmids (Table S1). SD-Leu-FoA (SD-Leu medium with 1 mg/mL 5-fluoroorotic acid) was used for the removal of the gRNA expression plasmids from engineered yeasts. Leu and Leu-Ura drop-out media were purchased from FunGenome (Beijing, China).

2.2. Plasmid construction

To construct the gene expression cassettes, two empty vectors (pUC20 and pZT110) were first prepared, and traditional restriction enzyme-based cloning was used for the construction of the gene expression cassettes. gRNA plasmids targeting different genomic sites were designed on CRISPRdirect (http://crispr.dbcls.jp/) and constructed using PCR and in-fusion cloning. The plasmids used in this study are listed in Supplementary Table 1.

Table 1
S. cerevisiae strains used in this study.

Strains	Host strains	Descriptions	Resources
CEN.PK2–1C		*MATa; his3D1; leu2-3_112; ura3-52; trp1-289*	EUROSCARF
ALA07	CEN.PK2–1C	*gal80*Δ; *gal1-7*Δ::T_{ADH1}-P_{GAL4}-*GAL4*-T_{CYC1}; *dpp1*Δ::T_{ADH1} -P_{GAL10}-P_{GAL1}-*hem 1*-T_{CYC1}; *lpp1*Δ: T_{ADH1}-*hemL*-P_{GAL10}-P_{GAL1}-*hemA*-T_{CYC1}; ARS308:T_{ADH1}-P_{GAL10}-P_{GAL1}-*ACO2*-T_{CYC1};	Our lab
C1	ALA07	*adh3*Δ::T_{ADH1}-*hem3*-P_{GAL10}-P_{GAL1}-*hem2*-T_{CYC1}-T_{PGK1}-P_{GAL10}-P_{GAL1}-T_{TPS1};	This study
C2	ALA07	*adh3*Δ::T_{ADH1}-*hem3*-P_{GAL10}-P_{GAL1}-*hem2*-T_{CYC1}-T_{PGK1}-P_{GAL10}-P_{GAL1}-*hem 12*-T_{TPS1};	This study
C3	ALA07	*adh3*Δ::T_{ADH1}-*hem3*-P_{GAL10}-P_{GAL1}-*hem2*-T_{CYC1}-T_{PGK1}-*hem4*-P_{GAL10}-P_{GAL1}-*hem 12*-T_{TPS1};	This study
C4	C3	YPRCdelta15Δ::T_{ADH1}-*hem3*-P_{GAL10}-P_{GAL1}-*hem2*-T_{CYC1}-T_{PGK1}-*hem4*-P_{GAL10}-P_{GAL1}-*hem 12*-T_{TPS1};	This study
M1	ALA07	ARS208Δ::T_{ADH1}-P_{GAL10}-P_{GAL1}-MLS-*hem2*-T_{CYC1};	This study
M2	ALA07	ARS208Δ::T_{ADH1}-*hem3*-MLS-P_{GAL10}-P_{GAL1}-MLS-*hem2*-T_{CYC1};	This study
M3	ALA07	ARS208Δ::T_{ADH1}-*hem3*-MLS-P_{GAL10}-P_{GAL1}-MLS-*hem2*-T_{CYC1}-T_{PGK1}-*hem4*-MLS-P_{GAL10}-P_{GAL1}-T_{TPS1};	This study
M4	ALA07	ARS208Δ::T_{ADH1}-*hem3*-MLS-P_{GAL10}-P_{GAL1}-MLS-*hem2*-T_{CYC1}-T_{PGK1}-*hem4*-MLS-P_{GAL10}-P_{GAL1}-MLS-*hem 12*-T_{TPS1};	This study
CM1	C4	ARS208Δ::T_{ADH1}-P_{GAL10}-P_{GAL1}-MLS-*hem2*-T_{CYC1};	This study
CM2	C4	ARS208Δ::T_{ADH1}-*hem3*-MLS-P_{GAL10}-P_{GAL1}-MLS-*hem2*-T_{CYC1};	This study
CM3	C4	ARS208Δ::T_{ADH1}-*hem3*-MLS-P_{GAL10}-P_{GAL1}-MLS-*hem2*-T_{CYC1}-T_{PGK1}-*hem4*-MLS-P_{GAL10}-P_{GAL1}-T_{TPS1};	This study
CM4	C4	ARS208Δ::T_{ADH1}-*hem3*-MLS-P_{GAL10}-P_{GAL1}-MLS-*hem2*-T_{CYC1}-T_{PGK1}-*hem4*-MLS-P_{GAL10}-P_{GAL1}-MLS-*hem 12*-T_{TPS1};	This study
CM5	CM4	ARS1622Δ::T_{ADH1}-*GSH2*-P_{GAL10}-P_{GAL1}-*GSH1*-T_{CYC1};	This study
CM6	CM4	ARS1622Δ::T_{ADH1}-P_{GAL10}-P_{GAL1}-*SOD2*-T_{CYC1};	This study
CM7	CM4	ARS1622Δ::T_{ADH1}-P_{GAL10}-P_{GAL1}-*CTA1*-T_{CYC1};	This study
CM8	CM4	ARS1622Δ::T_{ADH1}-*CTA1*-P_{GAL10}-P_{GAL1}-*SOD2*-T_{CYC1};	This study

2.3. Yeast strain construction

For the construction of each strain, the amplified upstream homologous arm, the downstream homologous arm, cassettes with no less than 500 bp overlap with the homologous arms and the gRNA plasmid were cotransformed into *S. cerevisiae* using the Frozen-EZ Yeast Transformation II ™ Kit (ZYMO RESEARCH, USA) and plated on SD-Leu-Ura solid media. Transformants were directly verified with colony PCR using KOD-ONE (TOYOBO, Japan). To achieve continuous gene editing, the engineered strains were cross-streaked on an SD-Leu-5-FoA plate to remove gRNA plasmids.

2.4. Coproporphyrin III extraction and quantification

The cells in 1 mL of culture were harvested by centrifugation (12,000 rpm for 10 min at 4 °C). The supernatant was used to detect the production of ALA and coproporphyrin III. The amount of ALA was quantified using a previously described method with modified Ehrlich's agent [29]. The amount of coproporphyrin III was quantified using high-performance liquid chromatography (HPLC; 1260 Infinity II, Agilent) instrument equipped with a diode array detector. An Eclipse XDB-C18 reverse-phase column (1.8 μm, 4.6 mm × 150 mm, Agilent) was used and absorbance at 400 nm was monitored. A linear gradient method of 20–95 % solvent A in B at 40 °C was used. Solvent A was a 10:90 (v/v) HPLC grade methanol: acetonitrile mixture, and solvent B was a 0.5 % (v/v) trifluoroacetic acid (TFA) in HPLC grade water. The flow rate was 1 mL/min for 40 min [30].

2.5. Assay of reactive oxygen species (ROS) levels

ROS were assessed using the nonfluorescent DCFH-DA probe, which can penetrate cells and is eventually oxidized by ROS to fluorescent DCF [31]. The yeast strains were incubated in 10 μM DCFH-DA at 30 °C for 30 min in darkness, and the fluorescence intensity was monitored with a fluorescence spectrophotometer (excitation = 488 nm, emission = 525 nm).

2.6. Fed-batch fermentation

The media used for fed-batch fermentation were composed of YPD, 8 g/L KH_2PO_4, 3 g/L $MgSO_4$, 0.72 g/L $ZnSO_4{\cdot}7H_2O$, 10 mL/L trace metal solution, and 12 mL/L vitamin solution. First, a single colony was inoculated into 5 mL YPD in a tube and precultured for 18 h of shaking incubation (220 rpm) at 30 °C. Then, the first precultured cells were inoculated into a 250 mL flask containing 15 mL YPD medium and cultured for 14 h with shaking (220 rpm) at 30 °C. The second precultured cells were inoculated in 500 mL flasks containing 100 mL YPD and cultured in a rotary shaker (220 rpm) at 30 °C. These cultures were grown for approximately 24 h, after which 10 % (vol/vol) of the seed cultures were inoculated into a 5 L bioreactor (Bai Lun, China) with 3 L of medium. Fermentation was performed at 30 °C, and the pH of the fermentation system was maintained at 5.0 with automatic feeding of 5 M ammonia hydroxide. The air flow ranged from 1 vvm to 2 vvm (air volume/working volume/min) and the dissolved oxygen concentration (dO_2) was controlled above 40 % saturation using an agitation cascade (200–850 rpm).

A two-stage fed-batch fermentation strategy was used in this study. In the first stage, a feeding solution containing 500 g/L D-glucose, 9 g/L KH_2PO_4, 2.5 g/L $MgSO_4$, 3.5 g/L K_2SO_4, 0.28 g/L Na_2SO_4, 10 ml/L trace metal solution and 12 ml/L vitamin solution, along with 10 g/L yeast extract and 20 g/L peptone as a nitrogen source was used to achieve rapid cell growth. When the D-glucose concentration in the batch culture decreased to 1 g/L, the feeding solution was supplied to adjust the residual glucose concentration between 1 g/L and 2 g/L. When the cell mass began to slowly increase (to the stationary phase), the first stage ended and the inducer galactose was added. In the second stage, in addition to the same mineral salts and trace elements contained in the feeding solution, 800 g/L glucose was added. This concentrated medium was used to induce the accumulation of heme. The ethanol concentration was constantly monitored by an ethanol electrode (Bai Lun, China) and was maintained at 5 g/L by adjusting the feeding rate.

3. Results and discussion

3.1. Enhancing CP III accumulation through cytoplasmic metabolic engineering

5-Aminolevulinate (ALA) can serve as a precursor for the synthesis of CP III, making it a crucial intermediate in the heme synthesis pathway. Through the sequential catalysis of porphobilinogen synthase (encoded by *HEM2*), hydroxymethylbilane synthase (encoded by *HEM3*), uroporphyrinogen-III synthase (encoded by *HEM4*), and uroporphyrinogen decarboxylase (encoded by *HEM12*), CP III can be efficiently synthesized (Fig. 1). To ensure an adequate supply of precursors for CP III biosynthesis, we utilized a previously constructed *S. cerevisiae* strain (ALA07) as the initial strain for constructing the CP III-producing strain (Table 1). This strain has demonstrated an effective capacity for metabolizing glucose to produce ALA at a level of 160.0 mg/L in a shake flask assessment (Fig. 2A).

The porphobilinogen synthase (encoded by *HEM2*), hydroxymethylbilane synthase (encoded by *HEM3*), are considered to be rate-limiting enzymes for heme synthesis in *S. cerevisiae* and the uroporphyrinogen decarboxylase (encoded by *HEM12*) might be the next rate-limiting step [20]. Thus, augmenting these genes can potentially have a positive impact on the accumulation of CP III. Consequently, one copy each of *HEM2*, *HEM3* was first integrated into the genome of the starting strain ALA07, generating strain C1. To test the effect of overexpression of *HEM12* on CP III synthesis, one copy each of *HEM2*, *HEM3*, and *HEM12* was integrated into the genome of the strain ALA07, generating strain C2. Fermentation showed that strain C1 and strain C2 accumulated CP III 6.5 ± 0.3 and 23.6 ± 0.8 mg/L, respectively (Fig. 2B). It was observed that the two strains significantly consumed the precursor ALA, resulting in titers dropping to 150.1 ± 3.7 and 119.0 ± 4.4 mg/L, respectively (Fig. 2A). Based on these results, an additional copy of the *HEM4* gene was integrated into the genome of strain C2 to evaluate the effect on the CP III product. Strain C3 also exhibited an increased CP III titer of 32.5 ± 0.5 mg/L, representing a significant improvement of approximately 37.7 % compared to that of the C2 strain (Fig. 2B).

To further increase the accumulation of CP III, the second copy of the expression cassettes for genes *HEM2*, *HEM3*, *HEM4* and *HEM12* was integrated into the genome of strain C3. However, the resulting strain C4 displayed a slight increase in the CP III titer compared to that of its parental strain C3, reaching 34.9 ± 0.2 mg/L (Fig. 2B). Moreover, the ALA titer of strain C4 was 96.6 ± 1.9 mg/L, which was slightly lower to that of strain C3 (100.1 ± 1.1 mg/L) (Fig. 2A). Increasing the copy number of pathway genes showed a limited increase in CP III production, indicating that the single cytoplasmic engineering could not efficiently utilize the full range of precursor ALA.

3.2. Increasing CP III accumulation through mitochondrial compartmentalization metabolic engineering

Mitochondria, which are the site of the TCA cycle, oxidative phosphorylation and energy metabolism, can provide an isolated environment with abundant precursors and increased redox potential [32]. ALA is primarily synthesized in mitochondria and then transported to the cytoplasm for the four-step enzymatic synthesis of CPG III, followed by spontaneous oxidation to form CP III. If a four-step CP III biosynthesis pathway was constructed in mitochondria, it should theoretically be possible to further increase its production due to direct conversion from ALA. To verify this hypothesis, the *HEM2*, *HEM3*, *HEM4* and *HEM12* genes were fused with the N-terminal mitochondrial localization signal

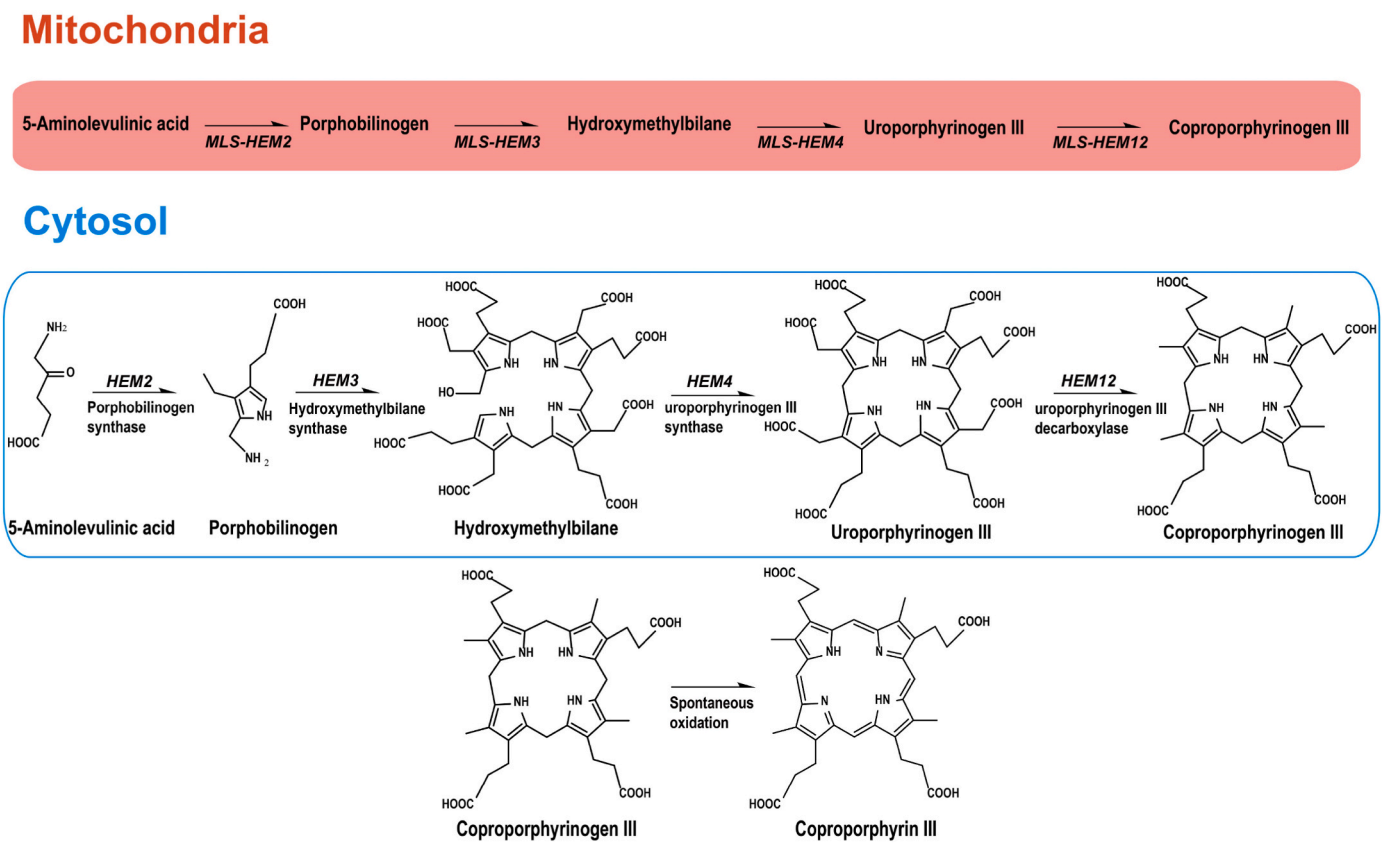

Fig. 1. Schematic diagram of CP III production by *S. cerevisiae*.

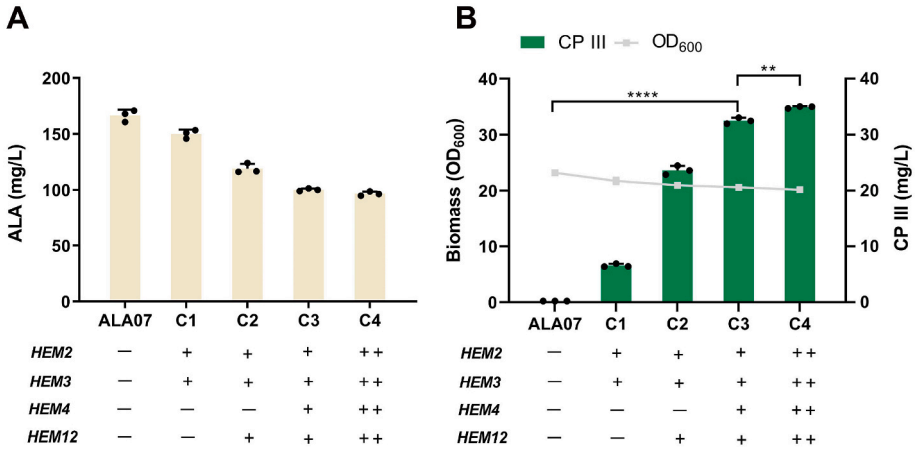

Fig. 2. Cytoplasmic metabolic engineering to enhance the CP III production. (A) ALA titers of the engineered strains. (B) The determination of CP III titers and maximum biomasses of the engineered strains. All data indicate the mean of three independent biological experiments. Error bars show standard deviation from three independent experiments.

(MLS) derived from subunit IV of cytochrome C oxidase (encoded by *Cox 4*) [24]. The precise localization performance of MLS for target proteins in mitochondria was examined using confocal scanning laser microscopy (CSLM) (Fig. 3A). Then, these genes were subsequently individually integrated into the genome of strain ALA07 to generate the recombinant strains M1, M2, M3 and M4 (Table 1).

As expected, strain M4 exhibited 10.7 ± 0.4 mg/L CP III after the introduction of all four fusion genes, indicating that synthesis by mitochondrial compartmentalization could indeed increase CP III production (Fig. 3B). However, the maximum biomass of strain M4 decreased by 13.8 % compared to that of the control strain ALA07. Furthermore, strains M1, M2, M3 and M4 reduced ALA accumulation by 2.4 %, 9.8 %, 16.4 % and 17.9 %, respectively (Fig. 3B), indicating that mitochondrial engineering alone may not be sufficient to significantly enhance the transformation of ALA precursors into the target product CP III. Nevertheless, these findings provided evidence that mitochondrial engineering can enhance the bioconversion of ALA to the target product CP III.

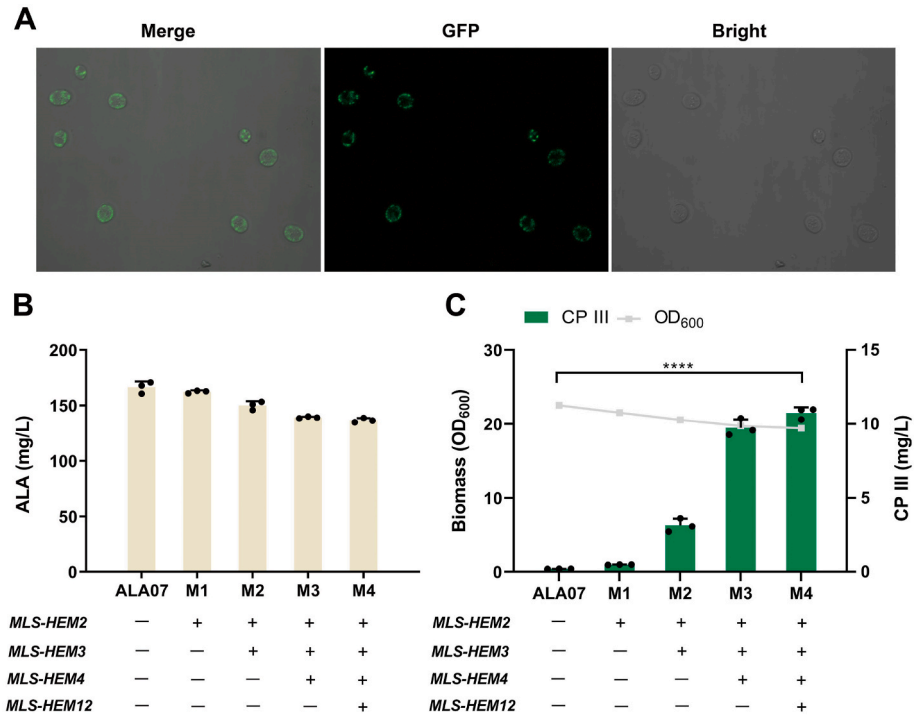

Fig. 3. CP III biosynthesis compartmentalized in the mitochondria of *S. cerevisiae*. (A) CSLM analysis of mitochondrial localization signal. (B) ALA titers of the engineered strains. (C) CP III titers and maximum biomasses of the engineered strains. All data indicate the mean of three independent biological experiments. Error bars show standard deviation from three independent experiments.

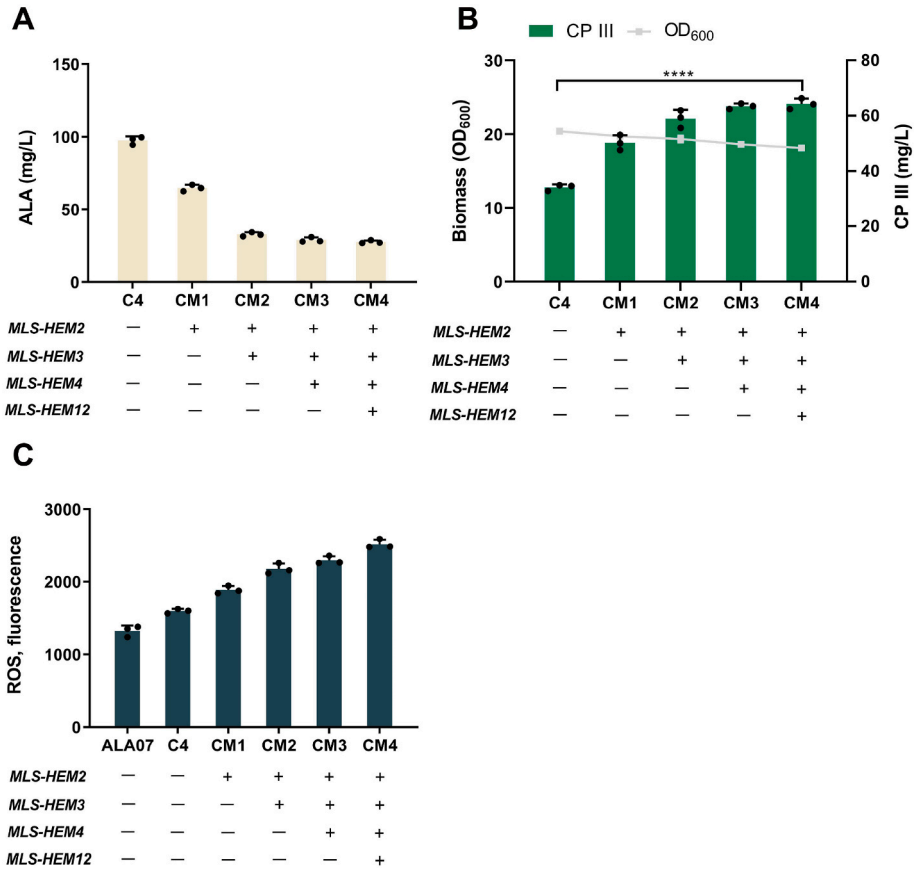

Fig. 4. Cytoplasmic and mitochondria engineering for the CP III overproduction. (A) ALA titers of the engineered strains. (B) CP III titers and maximum biomasses of the engineered strains. (C) ROS level of the engineered strains. All data indicate the mean of three independent biological experiments. Error bars show standard deviation from three independent experiments.

3.3. Combining cytoplasmic and mitochondrial metabolic engineering to enhance the accumulation of CP III

The previous experiment significantly increased the accumulation of the CP III by integrating an additional copy of the pathway genes into the genome. However, further increases in copy numbers did not yield significant improvements in product production. Based on these results, we attempted to further enhance CP III accumulation by combining cytoplasmic engineering with mitochondrial engineering. Consequently, we overexpressed the *HEM2* gene fused with the N-terminal MLS in strain C4, resulting in the engineered strain CM1.

According to the assessment results, CM1 strains that overexpressed MLS-*HEM2* produced a CP III titer of 50.2 ± 2.7 mg/L. Furthermore, when MLS-*HEM2* and MLS-*HEM3* were overexpressed, the constructed CM2 strain achieved a CP III titer of 59.0 ± 3.2 mg/L, representing a significant increase of 72.8 % compared to that of the C4 strain (Fig. 4B). The sequential introduction of the MLS-*HEM4* and MLS-*HEM12* genes into genome of strain CM2 resulted in strains CM3 and CM4, respectively, exhibiting CP III titers of 63.4 ± 1.0 mg/L and 64.3 ± 1.9 mg/L (Fig. 4B). In summary, strain CM4 demonstrated a CP III titer that was found to be 1.8 times greater than strain C4 after compartmentalizing an additional copy of the four pathway genes into the mitochondria. Notably, the biomass of the CM4 strain decreased by 11.2 % compared to that of the C4 strain, which exclusively underwent cytoplasmic metabolic engineering.

Mitochondrial compartmentalization and cytoplasmic metabolic engineering effectively promoted the accumulation of CP III, but also resulted in a significant reduction in biomass. This could be attributed to the increasing concentration of CP III, which leads to the buildup of certain substances such like heme that are unfavorable for cell growth. Excessive heme accumulation can increase ROS levels in mitochondria, triggering stress responses in cells and consequently affecting the growth of engineered strains [33,34]. In addition, the mitochondrial compartmentalization of the CP III synthesis pathway also increased the metabolic burden on mitochondria. To validate these hypothesizes, the ROS levels in the aforementioned engineered strains were analyzed. As shown in Fig. 4C, the ROS levels of strains CM1, CM2, CM3 and CM4 increased by 42.5 %, 64.4 %, 73.2 % and 90.0 %, respectively, compared to strain ALA07. Notably, strain CM4 demonstrated the highest ROS level among these strains, suggesting that the introduction of additional CP III pathway indeed led to an increase in ROS production.

3.4. Improving the growth and CP III accumulation of the engineered strain by reducing the intracellular ROS level

There are natural antioxidant pathways in microorganisms that serve as effective ways to counteract cell damage induced by ROS [35]. For instance, glutathione (GSH) is a widely employed antioxidant in medical and food applications [36,37]. GSH can be synthesized through two consecutive reactions catalyzed by γ-glutamylcysteine synthase (encoded by *GSH1*) and glutathione synthase (encoded by *GSH2*) (Fig. 5A). By augmenting the synthesis of glutathione, it becomes feasible to reduce cellular ROS levels, thereby improving cellular performance. Consequently, *GSH1* and *GSH2* were co-overexpressed in strain CM4 to generate strain CM5. The CP III titer of strain CM5 reached 64.7 ± 1.4 mg/L, which was a slight increase of 4.5 % compared to strain CM4 (Fig. 5C). The ROS level of strain CM5 decreased by 18.3 % and the biomass OD_{600} increased by 17.7 % (Fig. 5B).

ROS primarily consist of various components, including superoxide anion radicals, hydroxyl radicals and hydrogen peroxide. Among them, superoxide anion radicals are converted to hydrogen peroxide catalyzed by superoxide dismutase (SOD) and subsequently converted to water and oxygen catalyzed by catalase (CAT) [38,39]. To achieve effective quenching of ROS, we introduced the genes *SOD2* encoding superoxide

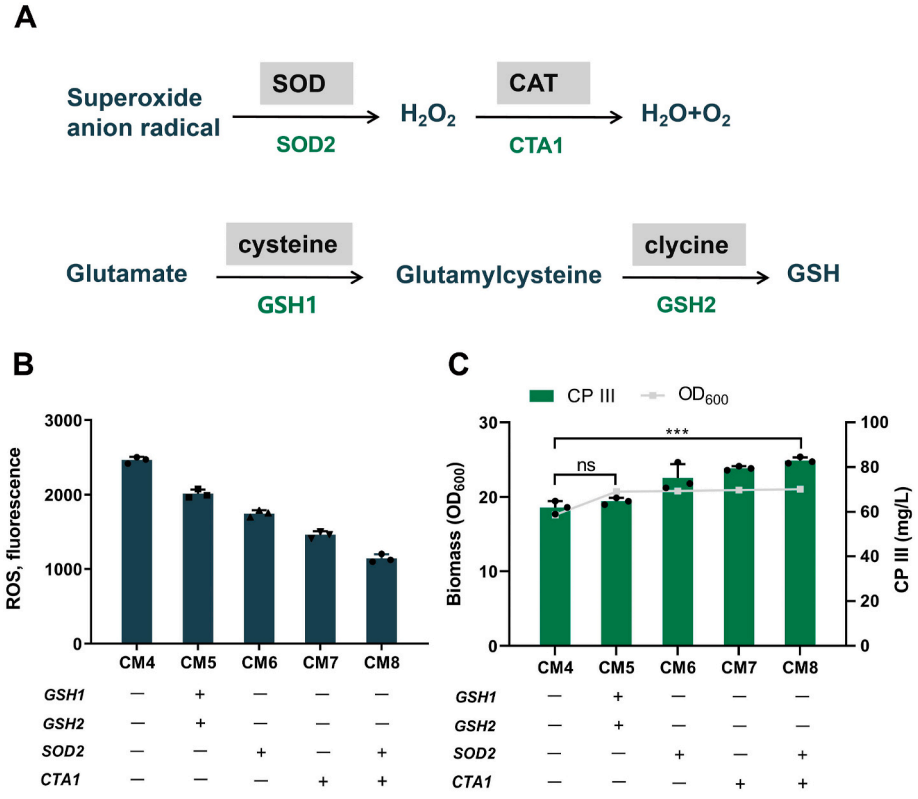

Fig. 5. Reducing the intracellular ROS level to improve the CP III production. (A) Augmentation of the glutathione pathway and ROS degradation pathway. (B) The ROS level in engineered strains. (C) CP III titers and maximum biomasses of the engineered strains. All data indicate the mean of three independent biological experiments. Error bars show standard deviation from three independent experiments.

dismutase and *CTA1* encoding catalase A (Fig. 5A) into strain CM4 to generate strains CM6 and CM7, respectively. Compared to strain CM4, the ROS levels of strains CM6 and CM7 were reduced by 29.1 % and 40.5 %, respectively (Fig. 5B). The two novel strains produced 75.2 ± 6.1 mg/L and 79.5 ± 0.9 mg/L CP III, representing increases of 17.3 % and 28.2 %, respectively, compared to their parental strain CM4 (Fig. 5C). Furthermore, the coaugmentation of *SOD2* and *CTA1* in the CM4 strain resulted in a synergistic increase in CP III accumulation, leading to an observed titer of 82.9 ± 1.4 mg/L in the obtained CM8 strain. Moreover, the growth of strains CM6, CM7, and CM8 was significantly improved, as evidenced by an increase in biomass OD_{600} of 18.2 %, 18.8 % and 19.6 %, respectively, compared to that of strain CM4 (Fig. 5C). These results suggested that enhancing the antioxidant system can effectively mitigate the level of ROS, thereby promoting cell growth as well as CP III accumulation.

3.5. Fed-batch fermentation for CP III production

The fed-batch fermentation performance of the constructed CM8 strain was assessed in a 5 L bioreactor. Two-stage fermentation was performed by using an optimized GAL regulatory system by *GAL80* complementation, which effectively separated the stages of cell growth and product synthesis. In the first stage, glucose was mainly used as a carbon source for cell growth, and the expression of pathway genes was repressed. In the second stage, after adding the galactose inducer, the cells began to accumulate CP III. During the feeding process, the concentration of glucose was controlled at a level below 2 g/L so that the amount of ethanol generated did not exceed 5 g/L. The highest CP III titer reached 402.8 ± 9.3 mg/L (Fig. 6), and the maximum OD_{600} was 149.7 after 132 h of fermentation. In other words, the time-space productivity of CP III in the CM8 strain reached 4.8 mg/L/h. These results demonstrated that the combination of cytoplasmic metabolic engineering and mitochondrial compartmentalization has a significant synergistic effect on enhancing the accumulation of the target product.

In *S. cerevisiae*, the precursor ALA of porphyrins is synthesized in the mitochondria and then transported to the cytoplasm for subsequent conversions [40]. Since mitochondrial compartmentalization can provide sufficient precursor, energy and cofactors for target product synthesis [28,41], it has been used for efficient production of squalene [28], geraniol [26], isoprene [42], and amorpha-4,11-diene [25]. After introducing an additional CP III synthetic pathway into the mitochondria, the engineered strain M4 displayed the expected increase in product accumulation. However, the mitochondrial engineered strain M4 exhibited a comparatively lower product enhancement effect than the cytoplasmic metabolic engineered strain, with a titer amounting to only 30 % of that observed for strain C4 (Fig. 3C). This result indicated that mitochondria may rapidly transport ALA precursors to the cytoplasm after synthesis, thus resulting in a very limited increase in the CP III titer by mitochondrial compartmentalization.

To optimize the utilization of ALA and enhance CP III accumulation, we combined cytoplasmic engineering and mitochondrial engineering to obtain a high-yield CP III yeast strain. However, the introduction of CP III synthesis pathway had a significant impact on cell growth, leading to a decrease in biomass (Fig. 3B). For example, compared to strain ALA07, strain CM4 exhibited a 30 % reduction in maximum biomass (Fig. 4B), which could be attributed to the accumulation of the downstream porphyrins of CP III, such as heme, and increased real-time metabolic flux within the mitochondria. Similar results have been observed in other studies of mitochondrial engineering [25,28,43]. Due to the accumulation of porphyrins in mitochondria, the level of cellular ROS increases, thereby impacting the growth of engineered strains [44,45]. To effectively mitigate the growth pressure resulting from the excessive accumulation of ROS in cells, the levels of key endogenous antioxidant enzymes were enhanced in engineered strains, leading to a substantial improvement in growth. This finding confirmed that reducing ROS accumulation by strengthening the antioxidant pathway genes is an effective strategy for alleviating the metabolic burden of mitochondrial engineering.

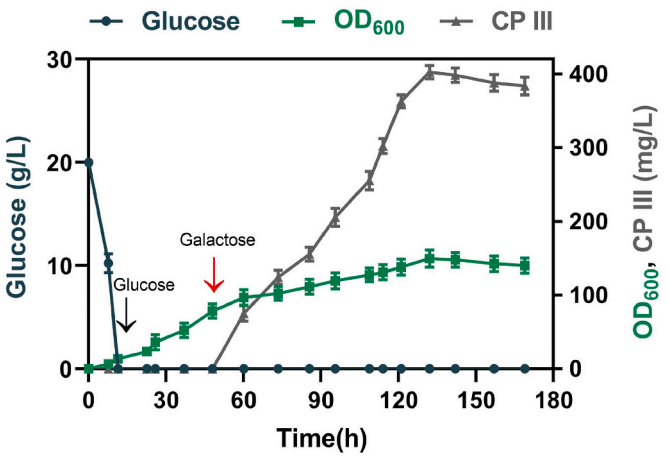

Fig. 6. Fed-batch fermentation of the CM8 strain for CP III production in a 5-L tank fermenter. The black arrow represents the feeding time of glucose into the medium. The red arrow represents the feeding time of galactose into the medium.

4. Conclusions

This study aimed to construct a cell factory capable of producing CP III by manipulating engineered strain of *S. cerevisiae* with an enhanced ALA synthesis pathway. By integrating an additional copy of genes involved in the CP III biosynthesis into the genome of the starting strain, we significantly increased the accumulation of the CP III to 32.5 ± 0.5 mg/L. However, increasing the copy number of pathway genes did not result in a sustained increase in CP III accumulation, while the synergistic enhancement of CP III production was achieved through the combined utilization of mitochondrial compartmentalization. The aforementioned strategy led to an elevation in intracellular ROS levels and impeded the growth of engineered strains. However, by augmenting antioxidant pathway genes such as *GSH1*, *GSH2*, *SOD2* and *CTA1* can significantly reduce ROS levels, thereby improving the synthesis of CP III. Ultimately, we successfully constructed an engineered strain that produced 82.9 ± 1.4 mg/L CP III in flask-shake cultivations and 402.8 ± 9.3 mg/L CP III in a 5.0-L bioreactor, using cytoplasmic engineering and mitochondrial compartmentalization. In conclusion, our study suggested that the use of mitochondria for porphyrin synthesis in *S. cerevisiae* is an effective strategy.

CRediT authorship contribution statement

Qidi Guo: Writing – original draft, Data curation, Formal analysis, Investigation, Methodology. **Jiaqi Xu:** Investigation. **Jiacun Li:** Data curation. **Shuyan Tang:** Software. **Yuhui Cheng:** Investigation. **Bei Gao:** Investigation. **Liang-Bin Xiong:** Writing – review & editing. **Jie Xiong:** Resources. **Feng-Qing Wang:** Funding acquisition, Writing – review & editing. **Dong-Zhi Wei:** Funding acquisition, Project administration.

Declaration of competing interest

The authors declare that there are no conflict of interests,we do not have any possible conflicts of interest.

Acknowledgments

This work is supported by the grant from the National Key Research and Development Program of China (2021YFC2100300), and 2023

Double World-class Project Key Program "Intelligent Biomanufacturing".

Appendix A. Supplementary data

Supplementary data to this article can be found online at https://doi.org/10.1016/j.synbio.2024.07.001.

References

[1] Dougherty TJ, Marcus SL. Photodynamic therapy. Eur J Cancer 1992;28A(10):1734–42. https://doi.org/10.1016/0959-8049(92)90080-l.

[2] Aviezer D, Cotton S, David M, Segev A, Khaselev N, Galili N, et al. Porphyrin analogues as novel antagonists of fibroblast growth factor and vascular endothelial growth factor receptor binding that inhibit endothelial cell proliferation, tumor progression, and metastasis. Cancer Res 2000;60(11):2973–80. https://doi.org/10.1530/acta.0.0440355.

[3] Cavaleiro JAS, Neves MGPM, Tomé AC, Silva AMS, Faustino MAF, Lacerda PS, et al. Porphyrin derivatives: synthesis and potential applications. J Heterocycl Chem 2000;37(3):527–34. https://doi.org/10.1002/jhet.5570370310.

[4] Zou QL, Abbas M, Zhao LY, Li SK, Shen GZ, Yan XH. Biological photothermal nanodots based on self-assembly of peptide-porphyrin conjugates for antitumor therapy. J Am Chem Soc 2017;139(5):1921–7. https://doi.org/10.1021/jacs.6b11382.

[5] Den Boer D, Li M, Habets T, Iavicoli P, Rowan AE, Nolte RJM, et al. Detection of different oxidation states of individual manganese porphyrins during their reaction with oxygen at a solid/liquid interface. Nat Chem 2013;5(7):621–7. https://doi.org/10.1038/NCHEM.1667.

[6] Mathew S, Yella A, Gao P, Humphry-Baker R, Curchod BFE, Ashari-Astani N, et al. Dye-sensitized solar cells with 13% efficiency achieved through the molecular engineering of porphyrin sensitizers. Nat Chem 2014;6(3):242–7. https://doi.org/10.1038/NCHEM.1861.

[7] Ryu WH, Gittleson FS, Thomsen JM, Li JY, Schwab MJ, Brudvig GW, et al. Heme biomolecule as redox mediator and oxygen shuttle for efficient charging of lithium-oxygen batteries. Nat Commun 2016;7:12925. https://doi.org/10.1038/ncomms12925.

[8] Carter KA, Shuai S, Hoopes MI, Luo D, Ahsan B, Grigoryants VM, et al. Porphyrin–phospholipid liposomes permeabilized by near-infrared light. Nat Commun 2014;5:3546. https://doi.org/10.1038/ncomms4546.

[9] Yella A, Lee HW, Tsao HN, Yi CY, Chandiran AK, Nazeeruddin MK, et al. Porphyrin-sensitized solar cells with cobalt (II/III)-based redox electrolyte exceed 12 percent efficiency. Science 2011;334(6056):629–34. https://doi.org/10.1126/science.1209688.

[10] Alibabaei L, Wang MK, Giovannetti R, Teuscher J, Di Censo D, Moser JE, et al. Application of Cu(II) and Zn(II) coproporphyrins as sensitizers for thin film dye sensitized solar cells. Energy Environ Sci 2010;3(7):956–61. https://doi.org/10.1039/b926726c.

[11] Chen L, Bai H, Xu JF, Wang S, Zhang X. Supramolecular porphyrin photosensitizers: controllable disguise and photoinduced activation of antibacterial behavior. ACS Appl Mater Interfaces 2017;9(16):13950–7. https://doi.org/10.1021/acsami.7b02611.

[12] Henriques CA, Pinto SMA, Aquino GLB, Pineiro M, Calvete MJF, Pereira MM. Ecofriendly porphyrin synthesis by using water under microwave irradiation. ChemSusChem 2014;7(10):2821–4. https://doi.org/10.1002/cssc.201402464.

[13] Bosca F, Tagliapietra S, Garino C, Cravotto G, Barge A. Extensive methodology screening of meso-tetrakys-(furan-2-yl)-porphyrin microwave-assisted synthesis. New J Chem 2016;40(3):2574–81. https://doi.org/10.1039/c5nj02888d.

[14] Lee SK, Chou H, Ham TS, Lee TS, Keasling JD. Metabolic engineering of microorganisms for biofuels production: from bugs to synthetic biology to fuels. Curr Opin Biotechnol 2008;19(6):556–63. https://doi.org/10.1016/j.copbio.2008.10.014.

[15] Chemler JA, Yan Y, Koffas MA. Biosynthesis of isoprenoids, polyunsaturated fatty acids and flavonoids in *Saccharomyces cerevisiae*. Microb Cell Factories 2006;5(1):20. https://doi.org/10.1186/1475-2859-5-20.

[16] Elke Nevoigt. Progress in metabolic engineering of *Saccharomyces cerevisiae*. Microbiol Mol Biol Rev 2008;72(3). https://doi.org/10.1128/mmbr.00025-07. 379-12.

[17] Hou J, Tyo K, Liu ZH, Petranovic D, Nielsen J. Engineering of vesicle trafficking improves heterologous protein secretion in *Saccharomyces cerevisiae*. Metab Eng 2012;14(2):120–7. https://doi.org/10.1016/j.ymben.2012.01.002.

[18] Hong KK, Nielsen J. Metabolic engineering of *Saccharomyces cerevisiae*: a key cell factory platform for future biorefineries. Cell Mol Life Sci 2012;69(16):2671–90. https://doi.org/10.1007/s00018-012-0945-1.

[19] Lian JZ, Zhao HM. Recent advances in biosynthesis of fatty acids derived products in *Saccharomyces cerevisiae* via enhanced supply of precursor metabolites. J Ind Microbiol Biotechnol 2015;42(3):437–51. https://doi.org/10.1007/s10295-014-1518-0.

[20] Hoffman M, Góra M, Rytka J. Identification of rate-limiting steps in yeast heme biosynthesis. Biochem Biophys Res Commun 2003;310(4):1247–53. https://doi.org/10.1016/j.bbrc.2003.09.151.

[21] Hara KY, Saito M, Kato H, Morikawa K, Kikukawa H, Nomura H, et al. 5-Aminolevulinic acid fermentation using engineered *Saccharomyces cerevisiae*. Microb Cell Factories 2019;18(1):194. https://doi.org/10.1186/s12934-019-1242-6.

[22] Malina C, Larsson C, Nielsen J. Yeast mitochondria: an overview of mitochondrial biology and the potential of mitochondrial systems biology. FEMS Yeast Res 2018;18(5):foy040. https://doi.org/10.1093/femsyr/foy040.

[23] Avalos JL, Fink GR, Stephanopoulos G. Compartmentalization of metabolic pathways in yeast mitochondria improves the production of branched-chain alcohols. Nat Biotechnol 2013;31(4):335–41. https://doi.org/10.1038/nbt.2509.

[24] Farhi M, Marhevka E, Masci T, Marcos E, Eyal Y, Ovadis M, et al. Harnessing yeast subcellular compartments for the production of plant terpenoids. Metab Eng 2011;13(5):474–81. https://doi.org/10.1016/j.ymben.2011.05.001.

[25] Yuan JF, Ching CB. Mitochondrial acetyl-CoA utilization pathway for terpenoid production. Metab Eng 2016;38:303–9. https://doi.org/10.1016/j.ymben.2016.07.008.

[26] Yee DA, DeNicola AB, Billingsley JM, Creso JG, Subrahmanyam V, Tang Y. Engineered mitochondrial production of monoterpenes in *Saccharomyces cerevisiae*. Metab Eng 2019;55:76–84. https://doi.org/10.1016/j.ymben.2019.06.004.

[27] Jia HJ, Chen TH, Qu JZ, Yao MD, Xiao WH, Wang Y, et al. Collaborative subcellular compartmentalization to improve GPP utilization and boost sabinene accumulation in *Saccharomyces cerevisiae*. Biochem Eng J 2020;164:107768. https://doi.org/10.1016/j.bej.2020.107768.

[28] Zhu ZT, Du MM, Gao B, Tao XY, Zhao M, Ren YH, et al. Metabolic compartmentalization in yeast mitochondria: burden and solution for squalene overproduction. Metab Eng 2021;68:232–45. https://doi.org/10.1016/j.ymben.2021.10.011.

[29] Zhao XR, Choi KR, Lee SY. Metabolic engineering of *Escherichia coli* for secretory production of free haem. Nat Catal 2018;1(9):720–8. https://doi.org/10.1038/s41929-018-0126-1.

[30] Ko YJ, Joo YC, Hyeon JE, Lee E, Lee ME, Seok J, et al. Biosynthesis of organic photosensitizer Zn-porphyrin by diphtheria toxin repressor (DtxR)-mediated global upregulation of engineered heme biosynthesis pathway in *Corynebacterium glutamicum*. Sci Rep 2018;8(1):14460. https://doi.org/10.1038/s41598-018-32854-9.

[31] Zhu CC, Chen JZ, Wang Y, Wang LX, Guo X, Chen N, et al. Enhancing 5-aminolevulinic acid tolerance and production by engineering the antioxidant defense system of *Escherichia coli*. Biotechnol Bioeng 2019;116(8):2018–28. https://doi.org/10.1002/bit.26981.

[32] Lian JZ, Mishra S, Zhao HM. Recent advances in metabolic engineering of *Saccharomyces cerevisiae*: new tools and their applications. Metab Eng 2018;50:85–108. https://doi.org/10.1016/j.ymben.2018.04.011.

[33] Guo YY, Zhao HL, Lin ZB, Ye TC, Xu DL, Zeng QC. Heme in cardiovascular diseases: a ubiquitous dangerous molecule worthy of vigilance. Front Cell Dev Biol 2021;9. https://doi.org/10.3389/fcell.2021.781839. 781-39.

[34] Sassa S. Why heme needs to be degraded to iron, biliverdin IXα, and carbon monoxide? Antioxidants Redox Signal 2004;6(5):819–24. https://doi.org/10.1089/ars.2004.6.819.

[35] Guan NZ, Li JH, Shin HD, Du GC, Chen J, Liu L. Microbial response to environmental stresses: from fundamental mechanisms to practical applications. Appl Microbiol Biotechnol 2017;101(10). https://doi.org/10.1007/s00253-017-8264-y. 3991-08.

[36] Penninckx MJ, Elskens MT. Metabolism and functions of glutathione in micro-organisms. Adv Microb Physiol 1993;34. https://doi.org/10.1016/s0065-2911(08)60031-4. 239-01.

[37] Ketterer B, Coles B, Meyer DJ. The role of glutathione in detoxication. Environ Health Perspect 1983;49:59–69. https://doi.org/10.1289/ehp.834959.

[38] Farrugia G, Bannister WH, Vassallo N, Balzan R. Aspirin-induced apoptosis of yeast cells is associated with mitochondrial superoxide radical accumulation and NAD(P)H oxidation. FEMS Yeast Res 2013;13(8):755–68. https://doi.org/10.1111/1567-1364.12075.

[39] Cuéllar-Cruz M, Castaño I, Arroyo-Helguera O, De Las Peñas A. Oxidative stress response to menadione and cumene hydroperoxide in the opportunistic fungal pathogen *Candida glabrata*. Memorias Do Instituto Oswaldo Cruz 2009;104(4):649–54. https://doi.org/10.1590/S0074-02762009000400020.

[40] Chelstowska A, Rytka J. Biosynthesis of heme in yeast *Saccharomyces cerevisiae*. Postepy Biochem 1993;39(3):173–85. https://doi.org/10.1007/s10529-014-1696-x.

[41] Yuan JF, Ching CB. Mitochondrial acetyl-CoA utilization pathway for terpenoid productions. Metab Eng 2016;38:303–9. https://doi.org/10.1016/j.ymben.2016.07.008.

[42] Yao Z, Zhou PP, Su BM, Su SS, Ye LD, Yu HW. Enhanced isoprene production by reconstruction of metabolic balance between strengthened precursor supply and improved isoprene synthase in *Saccharomyces cerevisiae*. ACS Synth Biol 2018;7(9):2308–16. https://doi.org/10.1021/acssynbio.8b00289.

[43] Lv XM, Wang F, Zhou PP, Ye LD, Xie WP, Xu HM, et al. Dual regulation of cytoplasmic and mitochondrial acetyl-CoA utilization for improved isoprene production in *Saccharomyces cerevisiae*. Nat Commun 2016;7:12851. https://doi.org/10.1038/ncomms12851.

[44] Tyo KEJ, Liu ZH, Petranovic D, Nielsen J. Imbalance of heterologous protein folding and disulfide bond formation rates yields runaway oxidative stress. BMC Biol 2012;10:16. https://doi.org/10.1186/1741-7007-10-16.

[45] Ishchuk OP, Frost AT, Muñiz-Paredes F, Matsumoto S, Laforge N, Eriksson NL, et al. Improved production of human hemoglobin in yeast by engineering hemoglobin degradation. Metab Eng 2021;66:259–67. https://doi.org/10.1016/j.ymben.2021.05.002.